

## Immune Distribution and Localization of Phosphoantigen-Specific V $\gamma$ 2V $\delta$ 2 T Cells in Lymphoid and Nonlymphoid Tissues in *Mycobacterium tuberculosis* Infection<sup>∇</sup>

Dan Huang,<sup>1</sup>† Yun Shen,<sup>1</sup>† Liyou Qiu,<sup>1</sup> Crystal Y. Chen,<sup>1</sup> Ling Shen,<sup>2</sup> Jim Estep,<sup>3</sup> Robert Hunt,<sup>3</sup> Daphne Vasconcelos,<sup>3</sup> George Du,<sup>1</sup> Pyone Aye,<sup>4</sup> Andrew A. Lackner,<sup>4</sup> Michelle H. Larsen,<sup>5</sup> William R. Jacobs, Jr.,<sup>5</sup> Barton F. Haynes,<sup>6</sup> Norman L. Letvin,<sup>2</sup> and Zheng W. Chen<sup>1\*</sup>

Department of Microbiology and Immunology, Center for Primate Biomedical Research, University of Illinois College of Medicine at Chicago, Chicago, Illinois<sup>1</sup>; Harvard Medical School, Beth Israel Deaconess Medical Center, Boston, Massachusetts<sup>2</sup>; Battelle Medical Research/Evaluation Facility, Battelle Memorial Institute, Columbus, Ohio<sup>3</sup>; Tulane National Primate Research Center, Covington, Louisiana<sup>4</sup>; Howard Hughes Medical Institute and Albert Einstein College of Medicine, New York, New York<sup>5</sup>; and Duke Human Vaccine Institute, Duke University, Durham, North Carolina<sup>6</sup>

Received 23 July 2007/Returned for modification 1 September 2007/Accepted 29 September 2007

Little is known about the immune distribution and localization of antigen-specific T cells in mucosal interfaces of tissues/organs during infection of humans. In this study, we made use of a macaque model of *Mycobacterium tuberculosis* infection to assess phosphoantigen-specific V $\gamma$ 2V $\delta$ 2 T cells regarding their tissue distribution, anatomical localization, and correlation with the presence or absence of tuberculosis (TB) lesions in lymphoid and nonlymphoid organs/tissues in the progression of severe pulmonary TB. Progression of pulmonary *M. tuberculosis* infection generated diverse distribution patterns of V $\gamma$ 2V $\delta$ 2 T cells, with remarkable accumulation of these cells in lungs, bronchial lymph nodes, spleens, and remote nonlymphoid organs but not in blood. Increased numbers of V $\gamma$ 2V $\delta$ 2 T cells in tissues were associated with *M. tuberculosis* infection but were independent of the severity of TB lesions. In lungs with apparent TB lesions, V $\gamma$ 2V $\delta$ 2 T cells were present within TB granulomas. In extrathoracic organs, V $\gamma$ 2V $\delta$ 2 T cells were localized in the interstitial compartment of nonlymphoid tissues, and the interstitial localization was present despite the absence of detectable TB lesions. Finally, V $\gamma$ 2V $\delta$ 2 T cells accumulated in tissues appeared to possess cytokine production function, since granzyme B was detectable in the  $\gamma\delta$  T cells present within granulomas. Thus, clonally expanded V $\gamma$ 2V $\delta$ 2 T cells appeared to undergo *trans*-endothelial migration, interstitial localization, and granuloma infiltration as immune responses to *M. tuberculosis* infection.

Accumulating evidence suggests that human  $\gamma\delta$  T cells belong to nonclassical T cells that contribute to both innate and adaptive immune responses. Resident  $\gamma\delta$  T cells within epithelia make up a portion of intraepithelial lymphocytes and may play a role in innate immunity against microbial invasions, immune surveillance of malignancies, and even skin repair after damage (1, 16). Peripheral  $\gamma\delta$  T cells circulating in the blood and lymphoid tissues appear to behave as both innate and adaptive immune cells (1, 5, 9, 16). Circulating V $\gamma$ 2V $\delta$ 2 T cells exist only in primates and, in humans, constitute 60 to 95% of total blood  $\gamma\delta$  T cells. Recent studies suggest that circulating V $\gamma$ 2V $\delta$ 2 T cells in primates can recognize phosphoantigens from some bacteria, such as *Mycobacterium tuberculosis*, and possess both innate and adaptive immune features (1, 5, 9, 16). The finding that “unprimed” V $\gamma$ 2V $\delta$ 2 T cells can recognize and react to wide ranges of nonpeptide ligands with the capability of “naïve” production of cytokines has been interpreted as a pattern recognition-like feature of innate immune cells.

On the other hand, the capacity of V $\gamma$ 2V $\delta$ 2 T cells to undergo major clonal expansion in primary infection and to mount rapid recall expansion upon reinfection has been proposed as an adaptive (memory-type) immune response of these  $\gamma\delta$  T cells (5). Consistent with these memory-type responses is the demonstration of memory phenotypes of V $\gamma$ 2V $\delta$ 2 T cells in the blood of humans (7).

Tuberculosis (TB) is the second leading cause of death worldwide, killing about 1.8 million persons annually. While human CD4 T cells play a crucial role in immune protection against *M. tuberculosis* infection, other T-cell populations, including V $\gamma$ 2V $\delta$ 2 T cells, are poorly characterized regarding their roles in immunity to TB. We recently demonstrated that *Mycobacterium bovis* BCG-vaccinated monkeys can mount memory-type immune responses of V $\gamma$ 2V $\delta$ 2 T cells in the pulmonary compartment following *M. tuberculosis* infection by aerosol and that the rapid recall responses of these  $\gamma\delta$  T cells coincide with protection against acutely fatal TB in juvenile rhesus monkeys (19). Nevertheless, immune responses of V $\gamma$ 2V $\delta$ 2 T cells in patients with chronic TB appear to be suppressed (for a review, see reference 4). It has been debated whether the depression of the V $\gamma$ 2V $\delta$ 2 T-cell response in TB is caused by the infection or allows the infection to progress (4). Further studies are needed to elucidate the biology and effector function of V $\gamma$ 2V $\delta$ 2 T cells in *M. tuberculosis* infection.

\* Corresponding author. Mailing address: Department of Microbiology and Immunology, Center for Primate Biomedical Research, University of Illinois College of Medicine at Chicago, 909 S. Wolcott Ave., MC790, Chicago, IL 60612. Phone: (312) 355-0531. Fax: (312) 996-6415. E-mail: zchen@uic.edu.

† The first two authors contributed equally to this work.

∇ Published ahead of print on 8 October 2007.

Little is known about the immune distribution and localization of antigen-specific T cells, including V $\gamma$ 2V $\delta$ 2 T cells, in mucosal interfaces of tissues/organs during infection of humans. Distribution patterns of V $\gamma$ 2V $\delta$ 2 T cells in lymphoid and nonlymphoid tissues/organs during TB have not been well described. Moreover, the anatomical localization of migrating V $\gamma$ 2V $\delta$ 2 T cells and their association with TB lesions remain largely unknown. Although  $\gamma\delta$  T cells in granulomatous reactions mediated by *Mycobacterium leprae* or *M. bovis* have been reported, the antigen specificity, immune trafficking, and source of these  $\gamma\delta$  T cells have not been defined (14, 20, 21). In this study, we made use of a macaque animal model of *M. tuberculosis* infection to assess V $\gamma$ 2V $\delta$ 2 T cells with regard to their tissue distribution, localization within tissues, and correlation with the presence or absence of TB lesions in lymphoid and nonlymphoid organs/tissues in the progression of severe pulmonary TB.

#### MATERIALS AND METHODS

**Macaque animals and *M. tuberculosis* infection.** A total of 11 monkeys, aged 2 to 6 years old, were included in these studies. Four rhesus (*Macaca mulatta*; animals 2717, 2722, 3055, and 2935) and three cynomolgus (*Macaca fascicularis*; animals FG16, FG14, and FG21) macaques were subjected to *M. tuberculosis* infection, and four healthy rhesus monkeys (animals 152, 155, 156, and 268) that received BCG vaccination 4 years earlier served as controls. At the time of the studies, BCG-vaccinated monkeys exhibited similar baselines of V $\gamma$ 2V $\delta$ 2 T cells to those of naïve animals. All animal protocols for the studies were IACUC approved. For *M. tuberculosis* infection, rhesus macaques were infected with *M. tuberculosis* strain H37Rv by aerosol, whereas cynomolgus monkeys were infected by bronchoscope-guided inoculation. The aerosol infection was done via a head-only inhalation system at the biosafety level 3 aerosol facility at Battelle Medical Research and Evaluation Facilities, Battelle Memorial Institute (19). The inhalation exposure system used to conduct the aerosol exposure tests was enclosed within a class III biological safety cabinet. The exposure system consisted of the following major components: an aerosol generation and delivery system, a sampling system, an exposure unit, and an exhaust system. A modified microbiological research establishment-type three-jet Collison nebulizer (BGI, Waltham, MA) with a precious fluid jar was used to generate a controlled delivery of *M. tuberculosis* aerosol (1- to 1.5- $\mu$ m-diameter droplets) from a phosphate-buffered saline (PBS) suspension. *M. tuberculosis* ( $10^6$  CFU/ml) was placed in the nebulizer, and monkeys were exposed for 10 min. Samples of the aerosol were collected using all-glass impingers (19) for analysis of the *M. tuberculosis* concentration (CFU/ml). The inhaled doses were determined based on the all-glass impinger concentration, sampler volume, sampling rate, and respiratory minute volumes of individual macaques. The inhaled doses for the individual monkeys ranged from 400 to 500 CFU of *M. tuberculosis*. After the *M. tuberculosis* aerosol challenge, the macaques were followed for the development of the acutely fatal form of TB, since rhesus macaques are extremely susceptible to acutely fatal TB. Four to 5 weeks after *M. tuberculosis* infection, one monkey was dying from respiratory stress and three others were moribund due to the progression of *M. tuberculosis* infection. The monkeys were immediately euthanized by a standard protocol for necropsy studies, and organs were carefully removed for immunologic and pathological evaluation. For the pulmonary infection of cynomolgus monkeys, 1,000 CFU of *M. tuberculosis* Erdman in 2 ml PBS was administered to each monkey by bronchoscope into the right caudal lung lobe, as previously described (13). Three cynomolgus macaques were moribund 11 weeks after pulmonary *M. tuberculosis* infection. They were subjected to necropsy for routine pathology and immunohistochemistry studies of organs to determine the anatomic localization of  $\gamma\delta$  T cells in relation to lesions in both the rhesus and cynomolgus monkeys. The studies of cynomolgus monkeys were done in a biosafety level 3 facility at the Tulane National Primate Research Center.

**Isolation of single-cell suspensions and lymphocytes from blood, lymphoid tissues, and nonlymphoid tissues from rhesus monkeys.** Peripheral blood lymphocytes were isolated from EDTA-blood of monkeys, using Ficoll-diatrizoate gradient centrifugation. Bone marrows were diluted in RPMI medium prior to isolation of lymphocytes by Ficoll-diatrizoate gradient centrifugation. The lymph nodes, thymus, and spleen were teased carefully to generate single-cell suspensions. Tissue pieces from livers, kidneys, and small/large intestinal mucosae were

minced in RPMI medium, as previously described (13, 18), to collect single-cell suspensions (mainly lymphocytes and tissue macrophages). The single-cell suspensions from these nonlymphoid organs were divided into three parts; one was used directly for mycobacterial CFU counts, one was saved directly as a pellet for real-time quantitation of *M. tuberculosis* Ag85B RNA, and one was subjected to isolation of lymphocytes by Ficoll-diatrizoate gradient centrifugation for flow cytometry-based analyses of  $\gamma\delta$  T cells.

**Flow cytometry analyses of V $\gamma$ 2V $\delta$ 2 T cells.** Rhesus lymphocytes isolated from the blood and lymphoid and nonlymphoid tissues and shipped overnight were stained immunologically with anti-V $\gamma$ 2, anti-V $\delta$ 2, anti-CD3, and anti-C $\delta$  (pan- $\gamma\delta$ ) antibodies, as described previously (24). Anti-human  $\gamma\delta$  monoclonal antibodies that cross-react with the corresponding macaque  $\gamma\delta^+$  T cells were used (24). Isotype-matched immunoglobulin or anti-V $\delta$ 3 in combination with other antibodies served as controls, as previously described (24).

**Enzyme-linked immunospot measurement of phosphoantigen-specific IFN- $\gamma$ -producing V $\gamma$ 2V $\delta$ 2 T cells.** Enzyme-linked immunospot assays for phosphoantigen-specific gamma interferon (IFN- $\gamma$ )-producing V $\gamma$ 2V $\delta$ 2 T cells were done as previously described (13, 17). The phosphoantigen isopentenyl pyrophosphate was purchased from Sigma (St. Louis, MO) and used at a working concentration of 15  $\mu$ M/liter.

**Bacterial CFU counts.** Viable mycobacterial infection levels in the blood, lung cells, and other tissue cells were determined by the quantitation of bacillus CFU in cell lysates from blood and tissue cells of *M. tuberculosis*-infected macaques, as previously described (19). For counts of bacillus organisms in the blood and bone marrow, 1 ml whole blood/diluted marrow was added to 10 ml red blood cell lysing buffer (Sigma R7757), incubated at room temperature for 15 min, and spun down by centrifugation at 1,500 rpm for 5 min. After decanting the supernatant, 0.5 ml of sterile water was added to the cell pellet to release intracellular mycobacteria. Three- or fivefold dilutions of the lysate were plated onto Middlebrook 7H11 agar plates (Difco). The plates were then incubated in a 37°C incubator for 3 weeks, and CFU were counted. Similarly, tissue single-cell suspensions comprised predominantly of  $\sim 10^6$  lymphocytes and macrophages (equivalent to 10 mg "lymphoid" tissue) were used for CFU counts of mycobacterial organisms. Cells from the tissues were pelleted and lysed with water prior to being plated and were incubated for 3 weeks on 7H11 agar plates as described above.

**Real-time quantitative PCR for quantitation of *M. tuberculosis* Ag85B mRNA.** *M. tuberculosis* mRNA was extracted from cell pellets frozen at  $-180^\circ\text{C}$  by using a TRIzol-based method (6), modified by ultrasonic disintegration. Eight hundred microliters of TRIzol (Invitrogen, Carlsbad, CA) was added to the cell pellet and then homogenized using ultrasonic disintegration by a model XL2000 sonicator (Misonix, Farmingdale, NY) to disrupt the walls and membranes of mycobacteria. The homogenized lysate was then subjected to phase separation and isolation of RNA. The extracted RNA was reverse transcribed to cDNA. The synthesized cDNA was used as a template to quantitate the expression of *M. tuberculosis* Ag85B RNA, which was done by real-time quantitative PCR using a TaqMan system on an ABI 7700 instrument (PE Biosystems, Foster City, CA). To normalize the expression of Ag85B RNA in the cells,  $\beta$ -actin mRNA was also quantitated as previously described (10, 25). The expression levels were expressed as mean copy numbers of Ag85B RNA in  $10^6$  equivalent cells (25). The methods and sequences of primers for PCR amplification of *M. tuberculosis* Ag85B mRNA were described previously (19).

**Gross and microscopic analyses of TB lesions and acid-fast staining.** Animals were sacrificed by barbiturate overdose and immediately subjected to necropsy. Multiple specimens from all tissues with gross lesions and remaining major organs were harvested. Specifically, each lobe of the lung, bronchial, mesenteric, axillary, and inguinal lymph nodes, tonsils, thymus, bone marrow, and other major organs were collected and labeled. Tissues were fixed in buffered 10% formalin with ionized zinc (Z-Fix; Anatech, Ltd., Battle Creek, MI) and frozen with and without Tissue-Tek OCT compound (Sakura Finetek USA, Inc., Torrance, CA). Gross lesions were enumerated for each tissue or estimated as a percentage of total organ involvement based on consolidation and discoloration, as viewed from the organ exterior and cut surfaces. Histologic specimens were embedded in paraffin and sectioned at 5  $\mu$ m for routine staining with hematoxylin and eosin and select staining with Ziehl-Neelsen acid-fast stain or Kinyoun's acid-fast stain. The severity of lung lesions was scored from 0 to 4 (0 = normal, 1 = focal granulomas, 2 = few microgranulomas, 3 = numerous granulomas, and 4 = grossly visible granulomas). The extent of lung involvement for each lung lobe was determined using digital scans of each lobe to record total pixel counts of hematoxylin- and eosin-stained material and the specimen area, measured in square cm, using Image-Pro Plus software (MediaCybernetics, Silver Spring, MD). Together, these data provide both the extent and severity of TB lesions.

**Immunohistochemistry analyses of V $\gamma$ 2V $\delta$ 2 T cells in tissues.** Standard protocols for immunohistochemical analyses were used to evaluate V $\gamma$ 2V $\delta$ 2 T cells in all tissue sections prepared from OCT-embedded and formalin-fixed tissues (22). Since almost all  $\gamma\delta$  T cells accumulated in tissues after *M. tuberculosis* infection were V $\gamma$ 2V $\delta$ 2 T cells but not other V $\delta$ 1 or V $\delta$ 3 T cells, we used anti-V $\delta$ 2 or anti-V $\gamma$ 2 antibody (Ab) in the immunohistochemistry analysis and interpreted V $\delta$ 2<sup>+</sup> or V $\gamma$ 2<sup>+</sup> cells as V $\gamma$ 2V $\delta$ 2 T cells in this study. Anti-V $\delta$ 2 (15D) and anti-V $\gamma$ 2 (7A9) were purchased from Pierce (Rockford, IL), and anti-V $\gamma$ 2(V $\gamma$ 9) 7B6 was provided by Marc Bonneville at INSERM U601, Nantes, France, and H el ene Sicard and Catherin Laplace at Innate Pharma, Marseilles, France.

A peroxidase-based visualization kit (EnVision system K1390; Dako, Carpinteria, CA) was used for immunohistochemical staining. The staining process for cryostat sections was performed as follows. Frozen specimens embedded in OCT were cut into 6- $\mu$ m-thick sections by use of a cryostat, fixed, permeabilized in cold acetone for 10 min, and washed in PBS. The sections were then treated for 5 min with 1% hydrogen peroxide in PBS to quench endogenous peroxidase, rinsed in PBS, blocked for 10 min with serum-free protein block (X0909; Dako), and rinsed in PBS. The sections were incubated with mouse anti-human V $\delta$ 2 Ab or anti-V $\gamma$ 2 Ab at a concentration of 4.8 mg/ml for 1 h at room temperature and then incubated for 30 min with peroxidase-labeled polymer-conjugated goat anti-mouse immunoglobulins. The sections were rinsed in PBS after each incubation, developed using 3,3'-diaminobenzidine chromogen solution as a substrate for 3 to 6 min, and counterstained with Gill's hematoxylin (Fisher Scientific) for 2 seconds. After dehydration in graded alcohols, sections were cleared in xylene and coverslipped.

For immunohistochemical staining of paraffin sections, 5- $\mu$ m-thick sections were generated from formalin-fixed paraffin-embedded tissues, using a conventional microtome. These tissue sections were incubated for 60 min at 56°C, deparaffinized in xylene for 40 min, rehydrated in graded ethanol solutions, and then transferred to PBS. The sections were stained following the procedures described above for cryostat sections.

**Two-color immunohistochemistry analyses of V $\gamma$ 2V $\delta$ 2 T effector cells.** Sections of formalin-fixed paraffin-embedded tissues were treated with Trilogy through pressure cooking for 5 min, transferred to hot target retrieval solution (Dako), and allowed to cool down. For V $\gamma$ 2/granzyme B staining, sections were blocked by peroxidase blocking reagent (Dako) and serum-free protein block (Dako) and then incubated for 1 h at room temperature with anti-V $\gamma$ 2 Ab (clone 7B6; 2 mg/ml) and subsequently for 30 min with peroxidase-conjugated goat anti-mouse immunoglobulin G (IgG). Brown staining was developed using 3,3'-diaminobenzidine chromogen solution as a substrate. The V $\gamma$ 2-stained sections were then blocked with DoubleBlock (Dako) and serum-free protein block and incubated for 1 h at room temperature with mouse anti-human granzyme B (clone GrB-7; Dako) (1:30 dilution). After being washed, the sections were incubated with biotinylated horse anti-mouse IgG (heavy plus light chains) (Vector) at a 1:200 dilution for 30 min and then ABC-AP (Vector) for 30 min. Granzyme B staining was identified with Vector Blue (Vector). Negative controls consisted of replacement of the primary antibody by an equivalent or greater concentration of mouse IgG1 (Dako) or normal goat serum. After dehydration in graded alcohols, sections were cleared in xylene and coverslipped. Images were captured with a Leica DSM LB2 microscope and DC 300 camera.

**Statistical analysis.** Multivariate analysis of variance and the Student *t* test were used, as previously described (18), to statistically analyze the data for differences in V $\gamma$ 2V $\delta$ 2 T-cell numbers or *M. tuberculosis* burdens between tissues/organs.

## RESULTS

**Immune distribution patterns of increases in V $\gamma$ 2V $\delta$ 2 T cells in the body in *M. tuberculosis* infection.** While almost all V $\gamma$ 2V $\delta$ 2 T cells expressing V $\gamma$ 2V $\delta$ 2 T-cell receptors (TCR) are specific for phosphoantigens (2, 23; data not shown), these  $\gamma\delta$  T cells appear to possess both innate and adaptive characteristics (1, 5, 9, 16). However, the immune distribution of these cells in lymphoid and nonlymphoid tissues/organs during their increases remains poorly characterized for infections. We presumed that pulmonary *M. tuberculosis* infection of naive monkeys would allow us to assess immune distribution patterns of V $\gamma$ 2V $\delta$ 2 T cells in peripheral blood and lymphoid tissues as well as the ability of these cells to migrate or accumulate in the

nonlymphoid tissues, including bacillus-challenged lungs with high TB burdens and extrathoracic remote organs with low or undetectable TB burdens. Rhesus monkeys were challenged with *M. tuberculosis* by aerosol and were euthanized for immediate collection of tissues/organs at the time the animals developed the severe form of pulmonary TB. Lymphocytes were isolated from both local and remote lymphoid and nonlymphoid organs/tissues and were assessed for the distribution of V $\gamma$ 2V $\delta$ 2 T cells. We evaluated the relative abundance of tissue V $\gamma$ 2V $\delta$ 2 T cells by measuring their percentages among total CD3<sup>+</sup> T cells, since earlier studies from us and others demonstrated that an increase in the percentage of antigen-specific T cells in a tissue/organ following clonal expansion correlated well with the increase in absolute number in the corresponding tissue/organ in early infections (11, 13, 19).

Marked increases in mean percentages of V $\gamma$ 2V $\delta$ 2 T cells were observed in lymphocytes from lungs and local bronchial lymph nodes of macaques euthanized with TB (Fig. 1). Some remote lymphoid organs/tissues (spleen and mesenteric lymph nodes) displayed statistically significant increases in mean percentages of V $\gamma$ 2V $\delta$ 2 T cells, whereas others (bone marrow and thymus) exhibited a subtle or no increase in the percentages of these  $\gamma\delta$  T cells (Fig. 1). Molecular analyses of V $\delta$ 2-D-J sequences suggested a polyclonal or oligoclonal distribution of V $\gamma$ 2V $\delta$ 2 T cells in the lymphoid and nonlymphoid tissues (19; data not shown). Interestingly, despite the increased numbers of V $\gamma$ 2V $\delta$ 2 T cells in the lymph nodes and spleen, there was no significant increase in the percentage or absolute number of V $\gamma$ 2V $\delta$ 2 T cells in the blood circulation at multiple time points after pulmonary *M. tuberculosis* infection of the monkeys (Fig. 1 and 2). However, the circulating V $\gamma$ 2V $\delta$ 2 T cells retained the capability to recognize phosphoantigen and produce IFN- $\gamma$  in response to in vitro phosphoantigen stimulation (Fig. 2b). The absence of V $\gamma$ 2V $\delta$ 2 T-cell expansion in the blood despite their accumulation in lymphoid organs appears to be inconsistent with the current paradigm for infection-driven proliferation of antigen-specific T cells, since clonal expansion of antigen-specific  $\alpha\beta$  T cells is usually seen in both the lymph nodes/spleen and blood circulation during early infections (3, 12, 15). This was also in contrast to the major expansion of blood V $\gamma$ 2V $\delta$ 2 T cells after intravenous BCG inoculation (4, 19).

Surprisingly, in extrathoracic remote nonlymphoid organs or tissues, there were striking increases in mean percentages of V $\gamma$ 2V $\delta$ 2 T cells for animals that were euthanized with TB disease and pulmonary *M. tuberculosis* infection. The V $\gamma$ 2V $\delta$ 2 T cells indeed accounted for up to 32% of CD3 T cells in lymphocytes isolated from the kidney, liver, and intestinal mucosae (intestines were described here as nonlymphoid, although they are considered nonclassical lymphoid tissue) (Fig. 1; Table 1). The increases in numbers of V $\gamma$ 2V $\delta$ 2 T cells in the kidney and intestinal mucosae were statistically greater than those in remote lymphoid tissues/organs, including mesenteric lymph nodes and the spleen (Fig. 1; Table 1). These data therefore demonstrated that the progression of pulmonary *M. tuberculosis* infection generated diverse patterns of immune distribution of V $\gamma$ 2V $\delta$ 2 T cells in various tissues. Notably, the percentage of V $\gamma$ 2V $\delta$ 2 T cells increased in lungs, bronchial lymph nodes, the spleen, and remote nonlymphoid organs but remained unchanged in the blood circulation during the progression of pulmonary TB.

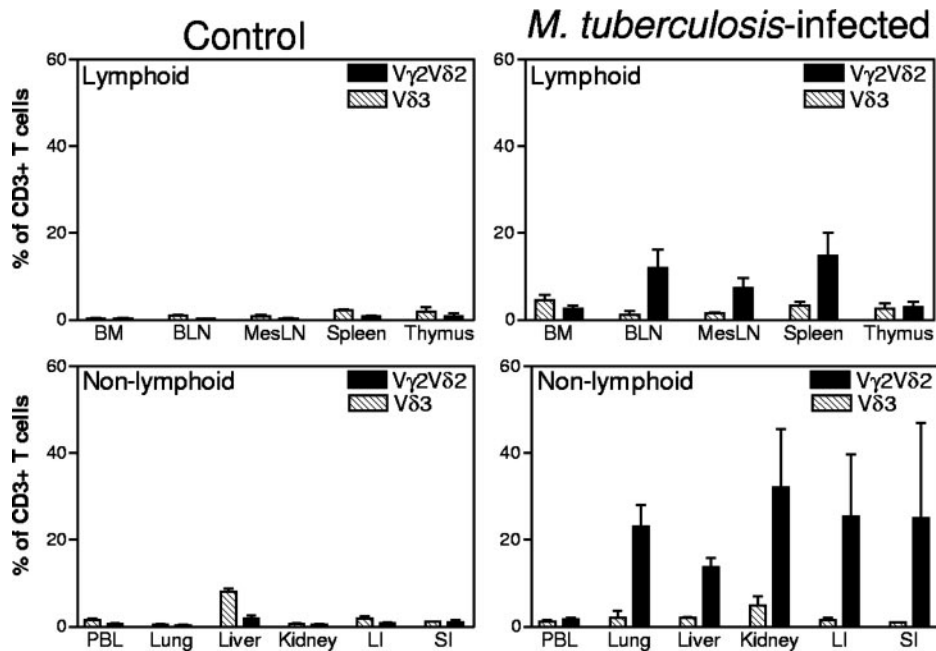


FIG. 1. Progression of pulmonary *M. tuberculosis* infection generated diverse patterns of immune distribution of clonally expanded V $\gamma$ 2V $\delta$ 2 T cells in the body, with remarkable accumulation of these cells in lymph nodes, spleens, lungs, and remote nonlymphoid organs but not in the blood. Shown are the mean percentages of V $\gamma$ 2V $\delta$ 2 T cells in lymphocytes isolated by Ficoll-diatrizoate gradient centrifugation from lymphoid (top) and nonlymphoid (bottom) tissues/organs after pulmonary *M. tuberculosis* infection. Error bars show standard deviations. Data were generated by flow cytometry analyses of tissues from four *M. tuberculosis*-infected rhesus monkeys and four previously BCG-vaccinated control rhesus monkeys. Except for the thymus, bone marrow (BM), and peripheral blood lymphocytes (PBL), *P* values were <0.01 when data between the *M. tuberculosis*-infected group and the control group were analyzed statistically. BLN, bronchial lymph nodes; MesLN, mesenteric lymph nodes; LI, large intestine; SI, small intestine.

**Increased numbers of V $\gamma$ 2V $\delta$ 2 T cells in tissues were associated with *M. tuberculosis* infection but independent of the severity of TB lesions.** Given the possibility that progression or dissemination of pulmonary *M. tuberculosis* infection induced the accumulation of V $\gamma$ 2V $\delta$ 2 T cells in local and remote organs, we sought to determine whether the increase in numbers of V $\gamma$ 2V $\delta$ 2 T cells was associated with the presence of bacterial burdens or TB lesions in those lymphoid and nonlymphoid

organs. Pulmonary *M. tuberculosis* infection generated high bacterial loads in lungs/bronchial lymph nodes and low bacterial loads in remote tissues/organs. Although bacillus organisms or *M. tuberculosis* mRNAs were detected in all organs (except for bone marrow), the lungs and local bronchial lymph nodes carried higher levels of bacteria (Table 1). However, the extent of bacterial infection or presence of TB lesions did not correlate with the magnitude of accumulation of V $\gamma$ 2V $\delta$ 2 T

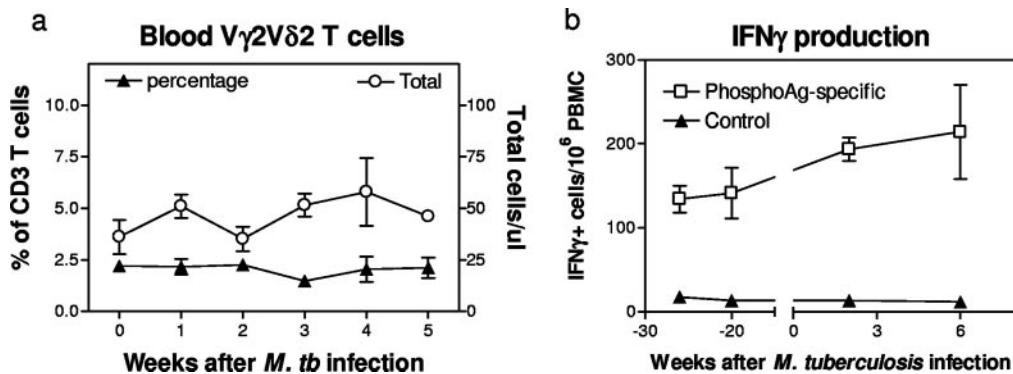


FIG. 2. There was no significant expansion of V $\gamma$ 2V $\delta$ 2 T cells in the blood circulation after pulmonary *M. tuberculosis* infection, despite remarkable increases in the numbers of these  $\gamma\delta$  T cells in lymphoid and nonlymphoid tissues/organs. (a) Percentages (left y axis) and absolute numbers (right y axis) of V $\gamma$ 2V $\delta$ 2 T cells in the blood of four rhesus monkeys after pulmonary *M. tuberculosis* infection. The slight increase in absolute numbers of V $\gamma$ 2V $\delta$ 2 T cells after the infection was not statistically significant (*P* > 0.05). (b) Subtle increase in numbers of isopentenyl pyrophosphate-specific IFN- $\gamma$ -producing V $\gamma$ 2V $\delta$ 2 T cells in the blood of three cynomolgus monkeys after *M. tuberculosis* infection. Note that circulating V $\gamma$ 2V $\delta$ 2 T cells maintained effector function for IFN- $\gamma$  production in response to in vitro stimulation with phosphoantigen, but not control glucose, during the early phase of *M. tuberculosis* infection.

TABLE 1. TB lesions and distribution/accumulation of V $\gamma$ 2V $\delta$ 2 T cells in organs/tissues of four rhesus monkeys with the severe form of tuberculosis<sup>a</sup>

| Tissue <sup>b</sup> | % V $\gamma$ 2V $\delta$ 2 T cells <sup>c</sup> | <i>M. tuberculosis</i> CFU <sup>c</sup> | <i>M. tuberculosis</i> mRNA level <sup>c</sup> | Gross and microscopic TB lesions  |
|---------------------|---|---|--|---|
| BM                  | 2.5 $\pm$ 0.7                                   | 1.0 $\pm$ 0.3                           | ND   |   |
| BLN                 | 11.9 $\pm$ 4.2                                  | 262 $\pm$ 102                           | 16,046 $\pm$ 3,156                             | Gross granulomas  |
| Mesenteric LN       | 7.3 $\pm$ 2.3                                   |   | 232 $\pm$ 89                                   | No apparent TB lesions  |
| Spleen              | 14.8 $\pm$ 5.3                                  | ND                                      | 101 $\pm$ 26                                   | Focal mild (micro) granulomas (<2 mm) seen in two monkeys   |
| Thymus              | 3.0 $\pm$ 1.2                                   | ND                                      | 235 $\pm$ 155                                  |   |
| Blood               | 1.8 $\pm$ 0.3                                   | 16.3 $\pm$ 13.3                         | 33 $\pm$ 23                                    |   |
| Lung                | 23.0 $\pm$ 5.1                                  | 535.5 $\pm$ 163.5                       | 7,122 $\pm$ 4,795                              | Numerous gross granulomas   |
| Liver               | 13.8 $\pm$ 2.2                                  | ND                                      | 430 $\pm$ 312                                  | One monkey showed two small granulomas at gross pathological evaluation; microscopic analysis showed 1 to 10 mild granulomas (<2 mm) in two monkeys and no lesions in the other two monkeys |
| Kidney              | 32.1 $\pm$ 13.4                                 | ND                                      | 121 $\pm$ 80                                   | No detectable TB lesions  |
| Intestine           | 25.3 $\pm$ 14.3                                 | ND                                      | 242 $\pm$ 164                                  | No detectable TB lesions  |

<sup>a</sup> Three cynomolgus monkeys were euthanized due to severe TB 11 weeks after pulmonary *M. tuberculosis* infection. Necropsies showed that there were numerous microgranulomas in the lungs and bronchial lymph nodes, with or without focal microgranulomas in the liver, spleen, kidneys, or intestinal mucosa.

<sup>b</sup> BM, bone marrow; BLN, bronchial lymph nodes; LN, lymph nodes.

<sup>c</sup> Data are means  $\pm$  standard deviations. ND, not done.

cells in the tissues (Table 1). In fact, a larger percentage of V $\gamma$ 2V $\delta$ 2 T cells accumulated in the remote organs, such as the liver, kidney, and intestinal mucosae, but these organs had lower levels of bacteria than the local *M. tuberculosis* infection sites, i.e., the lungs and bronchial lymph nodes (Table 1). In addition, no or mild TB lesions were seen in these remote nonclassical lymphoid organs. Although all the monkeys displayed severe TB lesions in the lungs, there were no gross lesions in kidneys, intestinal mucosae, or livers at the time that necropsy was performed (only one of four rhesus monkeys exhibited two microgranulomas in the liver) (Table 1). Therefore, these results demonstrated that while disseminated *M. tuberculosis* infection clearly was associated with increased numbers of V $\gamma$ 2V $\delta$ 2 T cells after pulmonary *M. tuberculosis* infection, TB lesions did not appear to determine the extent of migration or accumulation of V $\gamma$ 2V $\delta$ 2 T cells in extrathoracic nonlymphoid tissues.

**In the severe TB setting, V $\gamma$ 2V $\delta$ 2 T cells were present in TB lesions in lungs.** It is generally believed that resident  $\gamma\delta$  T cells lining dermal or mucosal epithelia do not constantly circulate or migrate and therefore may not be able to infiltrate lesions through *trans*-endothelial migration. However, it is not known whether antigen-specific V $\gamma$ 2V $\delta$ 2 T cells circulating in the blood and lymphatics can behave like circulating  $\alpha\beta$  T cells to be present in lesions in tissues during infection. To address this question, we undertook an immunohistochemistry-based analysis of V $\gamma$ 2V $\delta$ 2 T cells in granulomatous TB lesions in bacillus-exposed lungs that contained a high TB burden. Since almost all  $\gamma\delta$  T cells accumulated in tissues after *M. tuberculosis* infection were V $\gamma$ 2V $\delta$ 2 T cells, we used anti-V $\delta$ 2 or anti-V $\gamma$ 2 Ab in the immunohistochemistry analysis and interpreted V $\delta$ 2<sup>+</sup> or V $\gamma$ 2<sup>+</sup> cells as V $\gamma$ 2V $\delta$ 2 T cells in this study. V $\gamma$ 2V $\delta$ 2 T cells were present in granulomatous TB lesions in the lungs after *M. tuberculosis* infection of rhesus monkeys (Fig. 3). Similarly, the presence of V $\gamma$ 2V $\delta$ 2 T cells in TB lesions was also seen in the lung tissues collected from three cynomolgus macaques euthanized at the terminal stage of TB (Fig. 3). In contrast, undetectable or small numbers of V $\gamma$ 2V $\delta$ 2 T cells were seen in lung tissues with small *M. tuberculosis* burdens

(data not shown; see Fig. 5b). Taken together, these results from static pictures therefore implied that V $\gamma$ 2V $\delta$ 2 T cells could be present in TB granulomas.

**In extrathoracic organs with no or few TB lesions, V $\gamma$ 2V $\delta$ 2 T cells localized in the interstitial compartment of nonlymphoid tissues, despite the absence of detectable TB lesions.** Since the extrathoracic remote nonlymphoid organs harbored abundant V $\gamma$ 2V $\delta$ 2 T cells but no or very few TB lesions (Fig. 1; Table 1), we made use of this setting to examine the relationship between the accumulation or localization of V $\gamma$ 2V $\delta$ 2 T cells and the presence or absence of detectable TB lesions in the remote extrathoracic organs. V $\gamma$ 2V $\delta$ 2 T cells were localized in the interstitia of kidneys, livers, and intestinal mucosae in the infected rhesus monkeys (Fig. 4a). Importantly, detailed histological evaluation of the V $\gamma$ 2V $\delta$ 2 T-cell-distributed tissues showed no detectable TB lesions (Fig. 4a), and these tissues did not display any detectable acid-fast bacilli (data not shown). Moreover, extensive analyses of normal tissues of the kidney, liver, and gut from previously BCG-vaccinated healthy monkeys showed no interstitial infiltration of V $\gamma$ 2V $\delta$ 2 T cells, although other  $\gamma\delta$  T-cell subsets that do not express V $\gamma$ 2V $\delta$ 2 TCR were present in the gut-associated lymphoid tissues (Fig. 4b). The interstitial localization of V $\gamma$ 2V $\delta$ 2 T cells was also seen in the remote extrathoracic nonlymphoid organs from cynomolgus macaques after pulmonary *M. tuberculosis* infection (Fig. 4a). These data therefore provide histological evidence that V $\gamma$ 2V $\delta$ 2 T cells possess the capability to localize themselves in the interstitial compartment of extrathoracic nonlymphoid tissues/organs during disseminated *M. tuberculosis* infection and that the interstitial localization of V $\gamma$ 2V $\delta$ 2 T cells correlates with the absence of detectable TB lesions in extrathoracic nonlymphoid organs.

**V $\gamma$ 2V $\delta$ 2 T cells present in TB granulomas were able to produce the cytotoxic granule molecule granzyme B.** The detection of V $\gamma$ 2V $\delta$ 2 T cells in lungs and extrathoracic organs raised the issue of whether these  $\gamma\delta$  T cells possessed effector functions in cytokine production. To address this possibility, we employed two-color immunohistochemistry analyses to de-

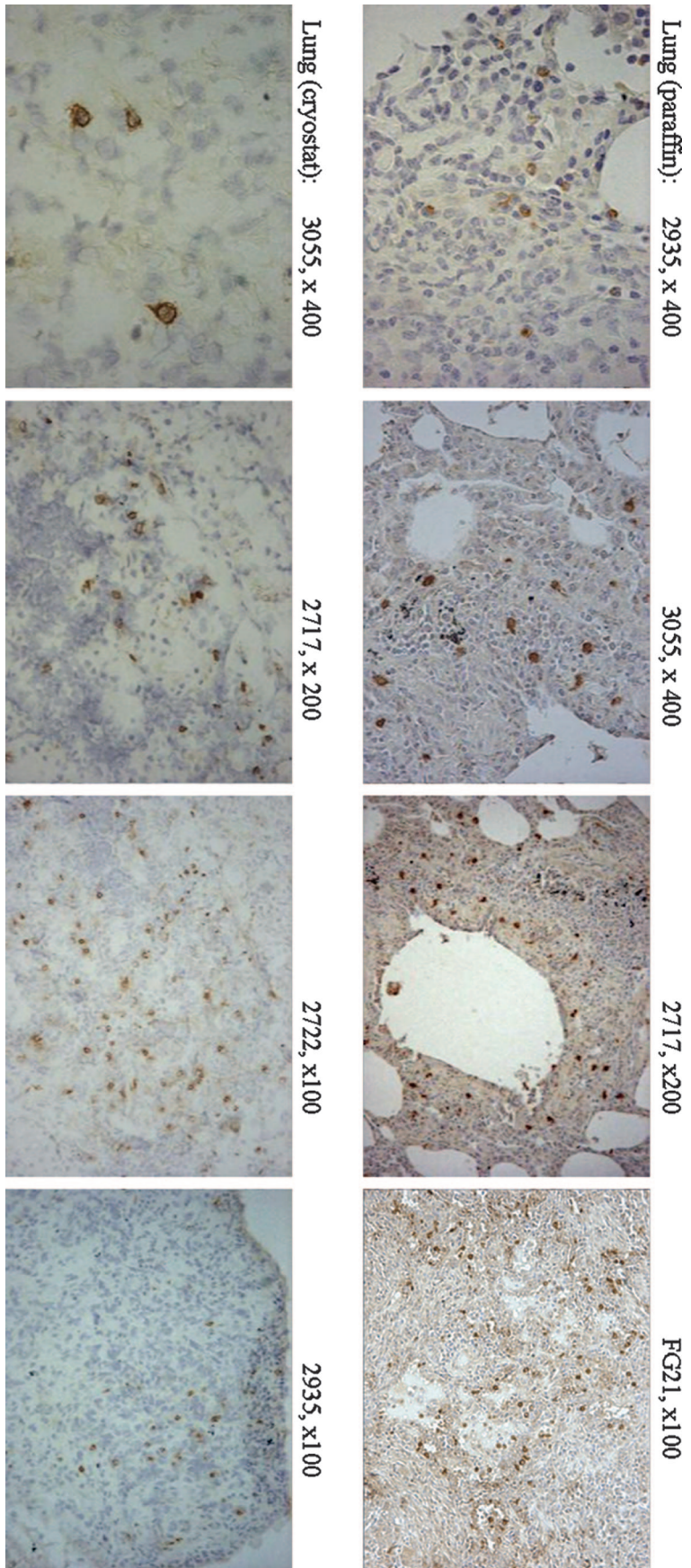


FIG. 3. In the severe TB lesion setting, V $\gamma$ 2V $\delta$ 2 T cells were present within TB granulomas in the lungs of rhesus monkeys euthanized with terminal TB. Both formalin-fixed (top) and frozen (bottom) lung tissue sections were analyzed by immunohistochemistry, using anti-V $\delta$ 2 Ab (for staining of cryostat sections) or anti-V $\gamma$ 2 Ab (for staining of formalin-fixed sections). The numbers in the upper right corner of each photo denote the individual monkey and the image magnification. Shown are representative photos of tissues from rhesus monkeys, except for animal FG21, which was one of three cynomolgus monkeys euthanized 11 weeks after pulmonary *M. tuberculosis* infection. In the lung sections derived from previously BCG-vaccinated healthy monkeys, no V $\delta$ 2<sup>+</sup> or V $\gamma$ 2<sup>+</sup> T cells were detected by immunohistochemistry analysis, as also shown in Fig. 4b. Negative staining was seen for an isotype IgG used as a control.

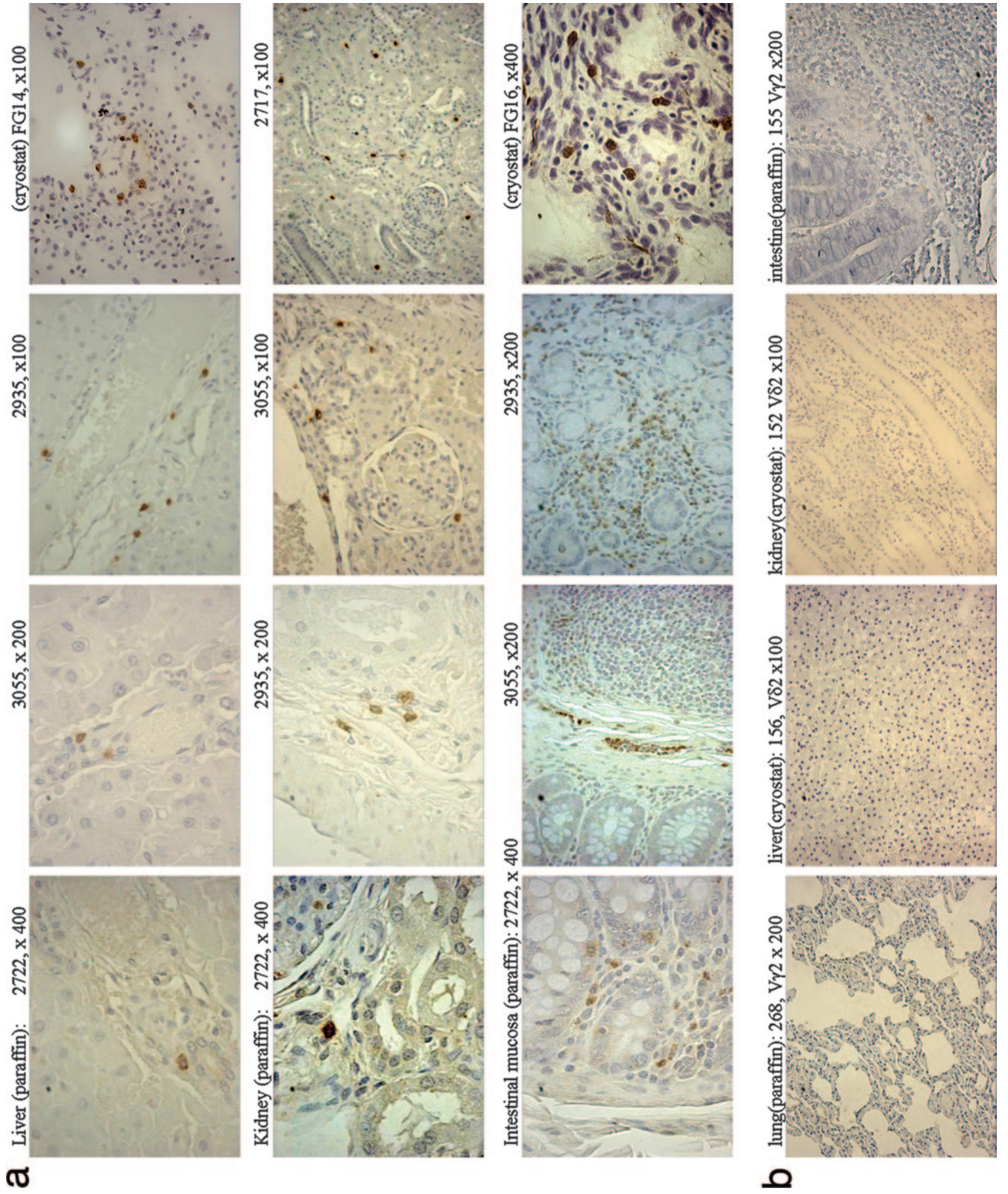


FIG. 4. (a) In extrathoracic organs with no or very few TB lesions, V $\gamma$ 2V $\delta$ 2 T cells migrated and localized in the interstitia of remote nonlymphoid organs, and such interstitial localization coincided with the absence of detectable TB lesions. Shown are representative photos of sections of the livers (top), kidneys (middle), and intestinal mucosae (bottom) from the studied animals. Note that the interstitial localization of V $\gamma$ 2 or V $\delta$ 2 T cells was seen in the sections of the remote organs but that there were no TB lesions or acid-fast bacilli detected in the sections. No apparent inflammation was seen in the sections. In the intestinal mucosa (crypts/lamina propria), V $\gamma$ 2 or V $\delta$ 2 T cells were mainly seen in the interstitium, and for monkey 3055, a number of V $\gamma$ 2 T cells appeared to emigrate or immigrate through the lymphatic vessels. Animals FG14 and FG16 were cynomolgus monkeys; the others were rhesus monkeys. (b) Representative photos derived from control experiments show that no or very few V $\delta$ 2<sup>+</sup> or V $\gamma$ 2<sup>+</sup> T cells could be detected in lung, liver, kidney, or intestinal mucosal tissue sections derived from healthy uninfected monkeys.

tect effector cytokines produced in situ by V $\gamma$ 2V $\delta$ 2 T cells accumulated in nonlymphoid tissues. Interestingly, a number of V $\gamma$ 2V $\delta$ 2 T cells within granulomas were able to produce the cytotoxic granule molecule granzyme B in the cytoplasm (Fig. 5a), although no IFN- $\gamma$  was detected in these  $\gamma\delta$  cells by using a stainable anti-IFN- $\gamma$  antibody (data not shown). The detectable granzyme B in V $\gamma$ 2V $\delta$ 2 T cells in tissues appeared to be driven by the *M. tuberculosis* burden, since granzyme B was not detectable in V $\gamma$ 2V $\delta$ 2 T cells localized in the noninflammatory areas next to the granulomas or in the “normal” granuloma-free tissues in lungs (Fig. 5b). There was no detectable granzyme B in V $\gamma$ 2V $\delta$ 2 T cells present in the extrathoracic organs/tissues in which no granulomatous inflammation was seen (data not shown). Thus, some V $\gamma$ 2V $\delta$ 2 T cells present in TB granulomas were able to produce detectable levels of granzyme B, suggesting that these cells might have an effector function in cytotoxic granule production.

## DISCUSSION

The current studies demonstrated that phosphoantigen-specific V $\gamma$ 2V $\delta$ 2 T cells not only expanded but also were distributed in nonlymphoid tissues/organs during the progression of pulmonary *M. tuberculosis* infection. The accumulation and localization of clonally expanded V $\gamma$ 2V $\delta$ 2 T cells in nonlymphoid organs, such as the lungs, kidneys, liver, and gut epithelial tissue (excluding the gut-associated lymphoid tissues), suggest that these cells undergo immune trafficking or tissue migration during TB. This scenario is supported by the paradigm that the nonlymphoid organs/tissues described above usually do not accommodate T-cell proliferation and expansion. The data from previously BCG-vaccinated healthy monkeys also indicate that V $\delta$ 2 or V $\gamma$ 2 T cells are almost undetectable by immunohistochemistry in those nonlymphoid tissues/organs and that only <2% of total T cells isolated from the tissues/organs are V $\gamma$ 2V $\delta$ 2 T cells.

Importantly, a number of V $\gamma$ 2V $\delta$ 2 T cells migrating to the lungs were able to produce granzyme B. The detectable granzyme B in V $\gamma$ 2V $\delta$ 2 T cells within TB granulomas suggests that these phosphoantigen-specific  $\gamma\delta$  T cells may indeed be effector immune cells with cytotoxic functions. Other V $\gamma$ 2V $\delta$ 2 T cells accumulated in tissues next to TB granulomas as well as in livers or kidneys might also have cytotoxic effector potential, although there was no detectable granzyme B in those cells. The reason why we cannot detect granzyme B in V $\gamma$ 2V $\delta$ 2 T cells localized in these nongranulomatous tissues may be due to the absence of a high *M. tuberculosis* burden in these areas. A high *M. tuberculosis* burden or TB lesions can result in the production of more phosphoantigen, which may activate migrating V $\gamma$ 2V $\delta$ 2 T cells further, to the extent that granzyme B is increased to a detectable level in these cells.

The pulmonary versus extrathoracic settings after the progression of pulmonary *M. tuberculosis* infection allowed us to elucidate the complex immune distribution and localization of clonally expanded V $\gamma$ 2V $\delta$ 2 T cells in tissues/organs of the body. The apparent TB lesions in the lungs and local lymph nodes make it possible to demonstrate that V $\gamma$ 2V $\delta$ 2 T cells can behave like their  $\alpha\beta$  T-cell counterparts and infiltrate TB granulomas as an immune response. However, such a severe TB setting clearly is not adequate for revealing a potential role of



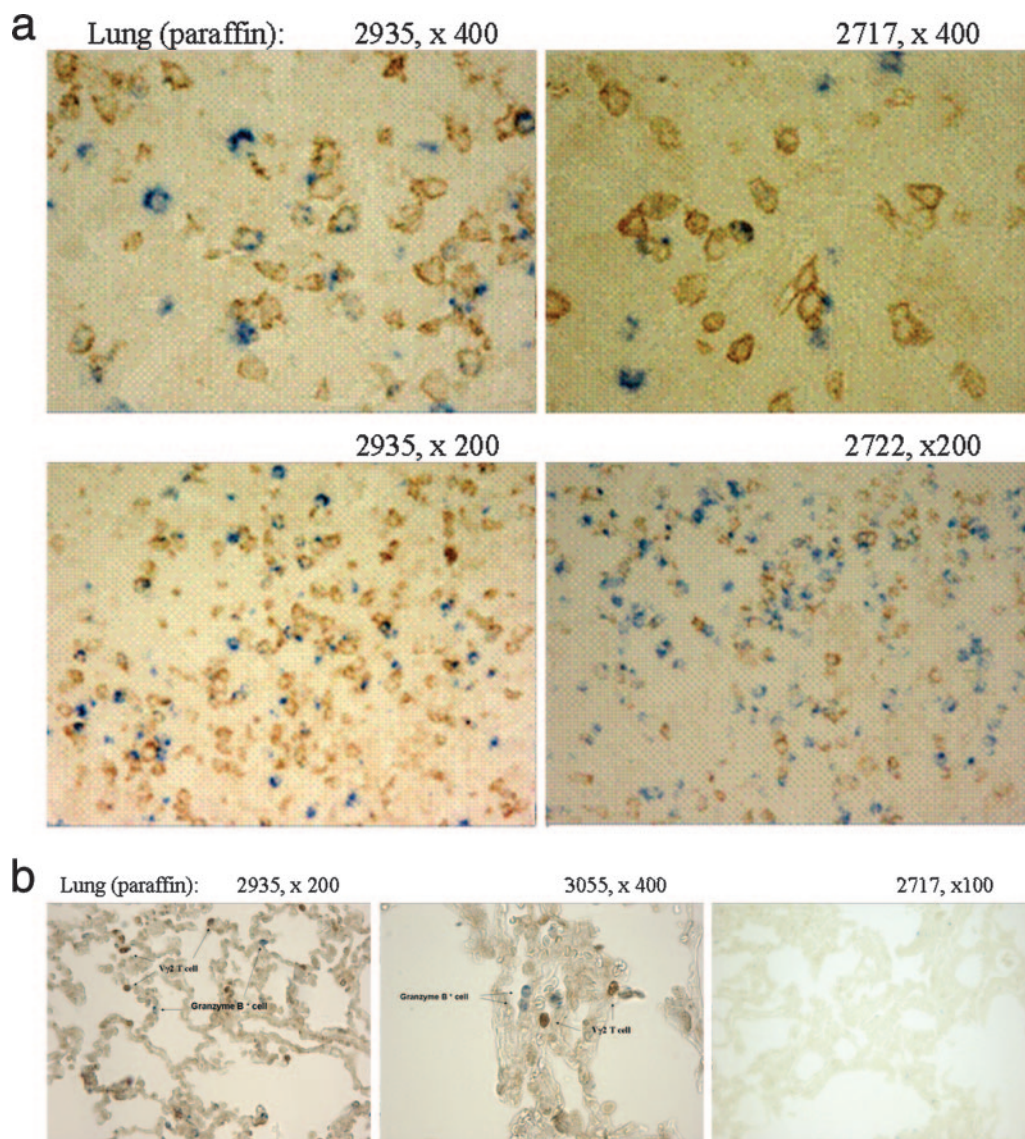


FIG. 5. Two-color immunohistochemistry analyses showed that V $\gamma$ 2V $\delta$ 2 T cells in TB granulomas were able to produce the cytotoxic granule molecule granzyme B. (a) A number of granzyme B-positive V $\gamma$ 2V $\delta$ 2 T cells were present in granulomas of lung sections derived from three representative rhesus monkeys with TB. Single brown-stained cells were V $\gamma$ 2V $\delta$ 2 T cells, whereas single blue-stained cells were granzyme B-positive cells. The random scanning and counting of 100 V $\gamma$ 2 T cells and 100 granzyme B-positive cells in the lung sections at a higher magnification ( $\times 400$ ) showed that approximately 29% of V $\gamma$ 2V $\delta$ 2 T cells in TB granulomas could express granzyme B and that about 9% of granzyme B-positive cells were indeed V $\gamma$ 2 T cells. (b) Very few or no granzyme B-positive V $\gamma$ 2V $\delta$ 2 T cells were seen in noninflammatory areas (left and middle panels), which were about 0.3 to 0.5 cm away from TB granulomas. Only singly stained cells, either V $\gamma$ 2V $\delta$ 2 T cells (brown) or granzyme B-positive cells (blue), were seen in these border areas. In the granuloma-free tissue section derived from the “normal” lung tissue (right), no V $\gamma$ 2V $\delta$ 2 T cells or granzyme B-positive cells were detected. Similar results were seen in the tissue sections from other monkeys. No granzyme B-positive cells were detected in the tissue sections derived from livers or kidneys of the monkeys (data not shown).

V $\gamma$ 2V $\delta$ 2 T cells in anti-TB responses in tissues. One can even argue that severe TB in the lung and subsequent *M. tuberculosis* dissemination may reflect a failure of infiltrating V $\gamma$ 2V $\delta$ 2 T cells and  $\alpha\beta$  T cells to contain the progression of pulmonary *M. tuberculosis* infection. In contrast, no or very few TB lesions in the extrathoracic tissues/organs provided an optimal setting in which to investigate the migration and distribution of phosphoantigen-specific V $\gamma$ 2V $\delta$ 2 T cells in response to low-level or undetectable infection in tissues. In this setting, we were able

to show tissue localization of migrated V $\gamma$ 2V $\delta$ 2 T cells and their presence despite the absence of TB lesions.

Despite the increases in numbers of V $\gamma$ 2V $\delta$ 2 T cells in lymphoid and nonlymphoid organs, no expansion of V $\gamma$ 2V $\delta$ 2 T cells was detected in the blood after *M. tuberculosis* infection of rhesus monkeys by the aerosol route. This finding is consistent with some reports describing the absence of V $\gamma$ 2V $\delta$ 2 T-cell expansion in the blood circulation in TB patients (for a review, see reference 4). In fact, it has been argued that depression of

the V $\gamma$ 2V $\delta$ 2 T-cell response in the blood of TB patients is an immune sequela of TB (4). However, it is important that blood V $\gamma$ 2V $\delta$ 2 T cells during the early phase of *M. tuberculosis* infection were still able to recognize phosphoantigen and produce IFN- $\gamma$  in response to in vitro phosphoantigen stimulation. In the current study, the precise mechanism underlying the lack of V $\gamma$ 2V $\delta$ 2 T-cell expansion in the blood during pulmonary *M. tuberculosis* infection is currently unknown. It is likely that the insufficient numbers of bacteria in the blood after pulmonary *M. tuberculosis* infection cannot produce a threshold level of phosphoantigen required for vigorous stimulation of clonal expansion of V $\gamma$ 2V $\delta$ 2 T cells, since infection-driven V $\gamma$ 2V $\delta$ 2 T-cell expansion is dependent upon the size of the mycobacterial inoculum (13). It is also possible that the large *M. tuberculosis* burdens in lungs and local lymph nodes induce marked inflammation and chemokine gradients that make blood V $\gamma$ 2V $\delta$ 2 T cells constantly migrate and accumulate in affected tissues and therefore result in the absence of apparent expansion of the blood V $\gamma$ 2V $\delta$ 2 T cells (4, 5).

It is important that V $\gamma$ 2V $\delta$ 2 T cells can migrate to and localize in the interstitial compartment of extrathoracic non-lymphoid tissues after pulmonary *M. tuberculosis* infection and that the interstitial localization of V $\gamma$ 2V $\delta$ 2 T cells is present despite the absence of detectable TB lesions or bacilli in these nonlymphoid organs. This finding suggests that the interstitial compartment in nonlymphoid tissues/organs may be the checkpoint for sensing or monitoring infection by V $\gamma$ 2V $\delta$ 2 T cells. Two possibilities may be considered to interpret the interstitial localization of clonally expanded V $\gamma$ 2V $\delta$ 2 T cells in extrathoracic tissues/organs. On the one hand, this may reflect the early immune trafficking of these circulating antigen-specific  $\gamma\delta$  T cells in response to the low TB burden after *M. tuberculosis* dissemination. With the progression of the local infection and tissue damage, these interstitial  $\gamma\delta$  T cells may migrate further and infiltrate potential TB lesions, as seen in bacillus-exposed lungs with high TB burdens. On the other hand, antigen-specific V $\gamma$ 2V $\delta$ 2 T cells localizing in the interstitium after migration may contribute to early protection or tissue homeostasis against TB lesions in these extrathoracic nonlymphoid organs/tissues with undetectable or low levels of *M. tuberculosis*. Since V $\gamma$ 2V $\delta$ 2 T cells within TB granulomas can produce granzyme B, there is reason to speculate that V $\gamma$ 2V $\delta$ 2 T cells localized at the interstitial compartment may potentially produce antimicrobial cytokines, such as IFN- $\gamma$  and bactericidal granulysin (8). This may limit *M. tuberculosis* replication and keep the area from infection/inflammation. Moreover, V $\gamma$ 2V $\delta$ 2 T cells migrating in the interstitial tissues can also produce tissue growth factors for homeostasis. These tissue growth factors may play a role in repairing tissue damage induced by *M. tuberculosis* (16).

Thus, our data suggest that V $\gamma$ 2V $\delta$ 2 T cells can readily undergo *trans*-endothelial migration, interstitial localization, and granuloma infiltration in response to *M. tuberculosis* infections. These antigen-specific V $\gamma$ 2V $\delta$ 2 T cells may contribute to immune responses or tissue homeostasis against TB.

#### ACKNOWLEDGMENTS

This work was supported by National Institutes of Health R01 grants HL64560 (to Z.W.C.) and RR13601 (to Z.W.C.) and by NCRB grant RR000164 (to TNPRC).

We thank Ken Williams at Harvard Medical School for technical advice for immunohistochemistry analysis, Marc Bonneville at INSERM U601, Nantes, France, and Innate Pharma, Marseilles, France, for providing the anti-V $\gamma$ 2 Ab (7B6) used in this study, and other members of Z. W. Chen's lab for technical assistance.

#### REFERENCES

- Born, W. K., C. L. Reardon, and R. L. O'Brien. 2006. The function of gammadelta T cells in innate immunity. *Curr. Opin. Immunol.* **18**:31–38.
- Bukowski, J. F., C. T. Morita, Y. Tanaka, B. R. Bloom, M. B. Brenner, and H. Band. 1995. V gamma 2V delta 2 TCR-dependent recognition of non-peptide antigens and Daudi cells analyzed by TCR gene transfer. *J. Immunol.* **154**:998–1006.
- Callan, M. F., N. Steven, P. Krausa, J. D. Wilson, P. A. Moss, G. M. Gillespie, J. I. Bell, A. B. Rickinson, and A. J. McMichael. 1996. Large clonal expansions of CD8+ T cells in acute infectious mononucleosis. *Nat. Med.* **2**:906–911.
- Chen, Z. W. 2005. Immune regulation of gammadelta T cell responses in mycobacterial infections. *Clin. Immunol.* **116**:202–207.
- Chen, Z. W., and N. L. Letvin. 2003. Adaptive immune response of Vgamma2Vdelta2 T cells: a new paradigm. *Trends Immunol.* **24**:213–219.
- Desjardin, L. E., M. D. Perkins, K. Wolski, S. Haun, L. Teixeira, Y. Chen, J. L. Johnson, J. J. Ellner, R. Dietze, J. Bates, M. D. Cave, and K. D. Eisenach. 1999. Measurement of sputum Mycobacterium tuberculosis messenger RNA as a surrogate for response to chemotherapy. *Am. J. Respir. Crit. Care Med.* **160**:203–210.
- Dieli, F., F. Poccia, M. Lipp, G. Sireci, N. Caccamo, C. Di Sano, and A. Salerno. 2003. Differentiation of effector/memory Vdelta2 T cells and migratory routes in lymph nodes or inflammatory sites. *J. Exp. Med.* **198**:391–397.
- Dieli, F., M. Troye-Blomberg, J. Ivanyi, J. J. Fournie, A. M. Krensky, M. Bonneville, M. A. Peyrat, N. Caccamo, G. Sireci, and A. Salerno. 2001. Granulysin-dependent killing of intracellular and extracellular Mycobacterium tuberculosis by Vgamma9/Vdelta2 T lymphocytes. *J. Infect. Dis.* **184**:1082–1085.
- Fournie, J. J., and M. Bonneville. 1996. Stimulation of gamma delta T cells by phosphoantigens. *Res. Immunol.* **147**:338–347.
- Huang, D., L. Qiu, R. Wang, X. Lai, G. Du, P. Sehgal, Y. Shen, L. Shao, L. Halliday, J. Fortman, L. Shen, N. L. Letvin, and Z. W. Chen. 2007. Immune gene networks of mycobacterial vaccine-elicited cellular responses and immunity. *J. Infect. Dis.* **195**:55–69.
- Kou, Z. C., M. Halloran, D. Lee-Parritz, L. Shen, M. Simon, P. K. Sehgal, Y. Shen, and Z. W. Chen. 1998. In vivo effects of a bacterial superantigen on macaque TCR repertoires. *J. Immunol.* **160**:5170–5180.
- Kuroda, M. J., J. E. Schmitz, W. A. Charini, C. E. Nickerson, C. I. Lord, M. A. Forman, and N. L. Letvin. 1999. Comparative analysis of cytotoxic T lymphocytes in lymph nodes and peripheral blood of simian immunodeficiency virus-infected rhesus monkeys. *J. Virol.* **73**:1573–1579.
- Lai, X., Y. Shen, D. Zhou, P. Sehgal, L. Shen, M. Simon, L. Qiu, N. L. Letvin, and Z. W. Chen. 2003. Immune biology of macaque lymphocyte populations during mycobacterial infection. *Clin. Exp. Immunol.* **133**:182–192.
- Modlin, R. L., C. Pirmez, F. M. Hofman, V. Torigan, K. Uyemura, T. H. Rea, B. R. Bloom, and M. B. Brenner. 1989. Lymphocytes bearing antigen-specific gamma delta T-cell receptors accumulate in human infectious disease lesions. *Nature* **339**:544–548.
- Pantaleo, G., H. Soudeyns, J. F. Demarest, M. Vaccarezza, C. Graziosi, S. Paolucci, M. B. Daucher, O. J. Cohen, F. Denis, W. E. Biddison, R. P. Sekaly, and A. S. Fauci. 1997. Accumulation of human immunodeficiency virus-specific cytotoxic T lymphocytes away from the predominant site of virus replication during primary infection. *Eur. J. Immunol.* **27**:3166–3173.
- Sharp, L. L., J. M. Jameson, D. A. Witherden, H. K. Komori, and W. L. Havran. 2005. Dendritic epidermal T-cell activation. *Crit. Rev. Immunol.* **25**:1–18.
- Shen, L., Y. Shen, D. Huang, L. Qiu, P. Sehgal, G. Z. Du, M. D. Miller, N. L. Letvin, and Z. W. Chen. 2004. Development of Vgamma2Vdelta2+ T cell responses during active mycobacterial coinfection of simian immunodeficiency virus-infected macaques requires control of viral infection and immune competence of CD4+ T cells. *J. Infect. Dis.* **190**:1438–1447.
- Shen, Y., L. Shen, P. Sehgal, D. Huang, L. Qiu, G. Du, N. L. Letvin, and Z. W. Chen. 2004. Clinical latency and reactivation of AIDS-related mycobacterial infections. *J. Virol.* **78**:14023–14032.
- Shen, Y., D. Zhou, L. Qiu, X. Lai, M. Simon, L. Shen, Z. Kou, Q. Wang, L. Jiang, J. Estep, R. Hunt, M. Clagett, P. K. Sehgal, Y. Li, X. Zeng, C. T. Morita, M. B. Brenner, N. L. Letvin, and Z. W. Chen. 2002. Adaptive immune response of Vgamma2Vdelta2+ T cells during mycobacterial infections. *Science* **295**:2255–2258.
- Tazi, A., I. Fajac, P. Soler, D. Valeyre, J. P. Ballesti, and A. J. Hance. 1991. Gamma/delta T-lymphocytes are not increased in number in granulomatous lesions of patients with tuberculosis or sarcoidosis. *Am. Rev. Respir. Dis.* **144**:1373–1375.

21. Wangoo, A., L. Johnson, J. Gough, R. Ackbar, S. Inglut, D. Hicks, Y. Spencer, G. Hewinson, and M. Vordermeier. 2005. Advanced granulomatous lesions in Mycobacterium bovis-infected cattle are associated with increased expression of type 1 procollagen, gammadelta (WC1+) T cells and CD68+ cells. *J. Comp. Pathol.* **133**:223–234.
22. Williams, K., A. Schwartz, S. Corey, M. Orandle, W. Kennedy, B. Thompson, X. Alvarez, C. Brown, S. Gartner, and A. Lackner. 2002. Proliferating cellular nuclear antigen expression as a marker of perivascular macrophages in simian immunodeficiency virus encephalitis. *Am. J. Pathol.* **161**:575–585.
23. Zhang, P. F., F. Cham, M. Dong, A. Choudhary, P. Bouma, Z. Zhang, Y. Shao, Y. R. Feng, L. Wang, N. Mathy, G. Voss, C. C. Broder, and G. V. Quinnan, Jr. 2007. Extensively cross-reactive anti-HIV-1 neutralizing antibodies induced by gp140 immunization. *Proc. Natl. Acad. Sci. USA* **104**:10193–10198.
24. Zhou, D., X. Lai, Y. Shen, P. Sehgal, L. Shen, M. Simon, L. Qiu, D. Huang, G. Z. Du, Q. Wang, N. L. Letvin, and Z. W. Chen. 2003. Inhibition of adaptive Vgamma2Vdelta2+ T-cell responses during active mycobacterial coinfection of simian immunodeficiency virus SIVmac-infected monkeys. *J. Virol.* **77**:2998–3006.
25. Zhou, D., Y. Shen, L. Chalifoux, D. Lee-Parritz, M. Simon, P. K. Sehgal, L. Zheng, M. Halloran, and Z. W. Chen. 1999. Mycobacterium bovis bacille Calmette-Guerin enhances pathogenicity of simian immunodeficiency virus infection and accelerates progression to AIDS in macaques: a role of persistent T cell activation in AIDS pathogenesis. *J. Immunol.* **162**:2204–2216.

---

*Editor:* A. J. Bäumlner